Chalcogenide Letters Vol. 18, No. 11, November 2021, p. 667 - 679

Numerical study of semi-transparent thin film heterojunction p-CuO/n-ZnO/AZO/ITO solar cells device model using SCAPS-1D

J. Husna[a,b], P. S. Menon[a], P. Chelvanathan[c,d *], M. A. Mohamed[a], S. K. Tripathy[e], T. R. Lenka[e]

[a]*Institute of Microengineering and Nanoelectronics (IMEN), Universiti Kebangsaan Malaysia (UKM), 43600 UKM Bangi, Selangor, Malaysia*

[b]*Department of Electrical Engineering, Islamic University of North Sumatra, Sumatera Utara 20217, Indonesia*

[c]*Solar Energy Research Institute (SERI), Universiti Kebangsaan Malaysia (UKM), 43600 UKM Bangi, Selangor, Malaysia*

[d]*Graphene & Advanced 2D Materials Research Group (GAMRG), School of Engineering and Technology, Sunway University, No. 5, Jalan Universiti, 47500 Bandar Sunway, Selangor, Malaysia*

[e]*Dept. of Electronics & Communication Engineering, National Institute of Technology Silchar, India*

In the current time, transparent and semitransparent solar cells in photovoltaic industry have drawn important attention owing to their potential use as solar windows, and energy harvesting devices for building, vehicle integration and flexible electronics. In this work, a semitransparent thin film heterojunction solar cells device structure of p-CuO/n-ZnO/AZO/ITO was numerically modeled using SCAPS-1D software tools. The cell's performance was investigated in terms of the different material layer properties, such as the thickness and carrier concentration or doping level. The simulation results of copper based semi-transparent thin film solar cell (TFSC) as the bottom cell model indicates that the highest efficiency was achieved at 8.9116 %, with the thickness and carrier concentration of n-ZnO material layer set at 20 nm, and 5.0 x 10^{18} cm^{-3} respectively, whereas the thickness of CuO absorber layer was fixed at 110 nm. Finally, the overall results show that CuO based absorber layer exhibits potential as photoactive material particularly for semitransparent thin film solar cells applications.

(Received June 22, 2021; Accepted November 1, 2021)

Keywords: Transparent/semitransparent thin film solar cells**,** Metal-Oxide semiconductor, ZnO, CuO, SCAPS-1D

1. Introduction

In over the last decade, transparent/semitransparent solar cells are being recognized as one of the promising technologies in the photovoltaic industry, which combines the benefits of the light absorption for photovoltaic conversion and the visible light transparency for functional and aesthetic applications, such as semitransparent photovoltaic windows, which are considered as a good solution for balancing the energy generation and visual comfort by integrating photovoltaic cells into the existing new buildings [1,2]. Photovoltaic technology can be classified into a few categories such as inorganic and organic [3,4–6], dye-sensitized solar cells [7], and the recently developed perovskite/hybrid perovskite solar cells [8].

Normally, the metallic and metal oxide coatings are deposited onto glass substrates with varying thickness with the purpose to control the amount of visible and infrared light that is reflected and transmitted [9]. Metal oxide compounds have been gaining wide research interest in the past years due to its multifunctional optoelectronics properties. Among those, Cu-based metal oxides binary compounds, namely, cupric oxide (CuO, tenorite) cuprous oxide (Cu_2O, cuprite), and Cu_4O_3 (paramelaconite) have been particularly rigorously investigated [10]. Both cupric oxide

* Corresponding author: cpuvaneswaran@ukm.edu.my

https://doi.org/10.15251/CL.2021.1811.667

(CuO) and cuprous oxide (Cu_2O) are categorized as a stable form of copper oxide compounds, and commonly used in thin film solar cell structure as a p-type photo-absorber layer [11-13]. Cupric oxide (CuO) has a monoclinic crystal structure, and it has band gap in the range of 1.0–2.1 eV [14-16]. Furthermore, the constituents of this material is non-toxic and cost effective and on the other hand the compound can be synthesized through relatively simple preparation process [17, 18]. Furthermore, CuO has a direct and indirect band gap [19, 20]. Normally, this metal oxide is widely used as a photo-absorber layer in photovoltaic devices structure [21–23]. Unlike CuO, Cu_2O metal oxide has a cubic crystal structure with a band gap in the range of 2–2.6 eV, hence, making it transparent to visible light spectrum. The highest power conversion efficiency (PCE) of Cu_2O-based solar cells is 8.1%, although the theoretical limit of PCE for Cu_2O solar cell is ~ 20% [24,25]. In past years, the metal oxide of Cu_2O has been used effectively for solar cell fabrication, and it was used in Schottky diode [26] and was proven experimentally. The performances of the solar cells are not as good as predicted in theoretical calculation due to the effect of some performance limiting factors such as the impurities, bulk defects, and the interface states. In the past few years, research in CuO-based heterojunction solar cells with the incorporation of other metal oxides has been conducted [27,28]. However, issues such as defect and the quality of photo-absorber film remains as the main constraining issues, which impedes the attainment higher PCE [29]. The PCE for thin-film heterojunction solar cell CuO-based device has been predicted that the PCE possible to reach up to 30%, by considering only radiative recombination [30].

The window layer is a very vital part of solar cell devices, as studies show that optimizing this layer could improve solar cell efficiency. Wide band-gap semiconductor materials play an important role as the window layer of TFSC in terms of optimizing the spectral response in short wavelengths area. Photons that are absorbed by a low band gap window layer material will not generate any photocurrent due to its poor response to the shortwave solar spectrum. Since over last decade, where both doped Zinc oxide and undoped ZnO films have been used in thin-film solar cells structure as the window layer. As well known, ZnO is a transparent metal oxide material that has a band gap energy value of 3.34 eV. In addition, it also has potential to be used in other optoelectronics electronic devices, due to its transparency in the visible spectral region [30,31], and the controllable n-type feature, excitonic properties, has enabled extensive usage in heterojunction thin film solar cells [32]. The presence of the absorber and buffer/window layer in thin-film solar structure gives rise to the interface defects between buffer and window layer which finally can influence to the performance solar cell devices [33]. In the purpose of overcoming the issue of band offset, a variant of doping and the varying thickness of material for each layer have vital contributions and play in controlling the performance of the cell, as presented for the diode in case of recombination-limited operation [34,35].

SCAPS-1D software is used to simulate different types of thin-film solar cells device such as CdTe, Cu(In,Ga)Se_2/CIGS, and some other heterojunction solar cells devices as well [36]. In this work, the numerical simulation of heterojunction solar cells of the p-CuO/n-ZnO/AZO/ ITO structure device was executed using SCAPS-1D, in an initial attempt to achieve the optimized parameter for metal oxide of the active layer (p/n type) set up. Furthermore, the main goal of this work is to achieve the higher power conversation efficiency (PCE) of semitransparent thin films heterojunction solar cell devices. SCAPS-1D is a familiar software and well known as one of the numerical tools for solving the problem in thin-film solar cells structure device by implementing the two continuity equations and the Poisson's equation [38]. In this work, we investigated some specific parameters such as layer thickness and concentration variation/doping level of semitransparent thin-film heterojunction solar cells structure p-CuO/n-ZnO/AZO/ ITO device, with the aim to see its effect in the solar cells device performance (Jsc, Voc, η, and FF).

2. Methods

SCAPS-1D or known as Solar Cell Capacitance Simulator is one of the modeling tools in a photovoltaic system and is generally known as one of free software as introduced by Burgelman et al in 1996, which is the SCAPS version that used for this simulation study is the SCAPS-1D 3.3.0. The semitransparent thin film CuO based solar cell device has simulated under the illumination of the standard; AM 1.5 G, 100 mW/cm^2, and the temperature at 300 K, and the details of the schematic/structure devices of p-CuO/n-ZnO/AZO/ ITO heterojunction solar cell has been presented and as described in Fig.1. Meanwhile, the material properties/parameters of the that used in this work including front and back contacts are provided as clearly shown in the table. 1 and 2. Poisso equation is given as below.

$$\frac{dE}{\partial x} = \frac{\rho}{\varepsilon} = \frac{q}{\varepsilon}(p(x) - n(x) - N_A + N_D) \quad (1)$$

where E is the electric field, ρ is the charge density and ε is the material permittivity. This equation gives the basic relationship between charge and electric field strength, meanwhile p(x), n(x), N_A and N_D are hole density, electron density, acceptor atom density and donor atom density, respectively. Furthermore, for the continuity equations of electrons and holes as expressed in the following equation;

$$\Delta.J_p = q(G - R) \quad (2)$$

$$\Delta.J_n = q(R - G) \quad (3)$$

where, G is the generation rate R is the recombination rate; J_p and J_n electron and hole current densities are respectively

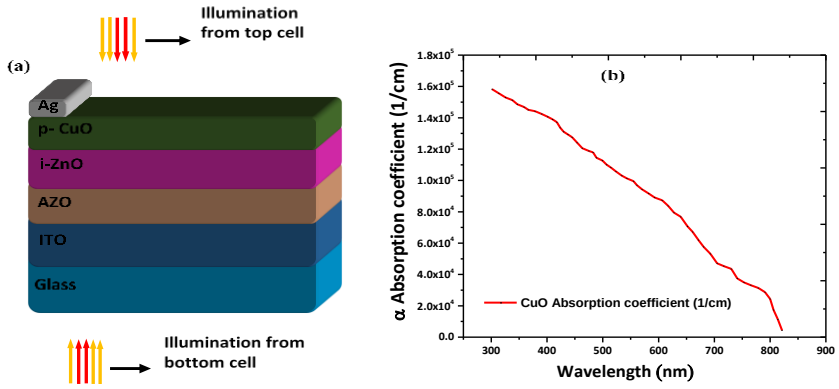

Fig. 1. (a) Semi-transparent TFSC CuO based device structure, and (b) The absorption coefficient of p-CuO Absorber Material Curve.

Table 1. Parameters of ZnO, CuO, and AZO that used in SCAPS simulation

Parameters	n-ZnO	p-CuO	AZO
Thickness (nm)	10-300	10-110	200
bandgap (eV)	3.400	1.5	3.300
electron affinity (eV)	4.1	4.070	4.450
dielectric permittivity (relative)	10	18.100	9
CB effective density of states ($1/cm^3$)	$4.0x10^{18}$	$2.2x10^{19}$	$2.2x10^{18}$
VB effective density of states ($1/cm^{3)}$	$9.0x10^{18}$	$5.5x10^{20}$	$1.8x10^{19}$
electron thermal velocity (cm/s)	$1.0x10^{7}$	$1.0x10^{7}$	$1.0x10^{7}$
hole thermal velocity (cm/s)	$1.0x10^{7}$	$1.0x10^{7}$	$1.0x10^{7}$
electron mobility (cm^2/Vs)	$5.0x10^{1}$	$1.0x10^{2}$	$1.0x10^{2}$
hole mobility (cm^2/Vs)	$2.0x10^{1}$	$1.0x10^{-1}$	$2.5x10^{1}$
shallow uniform donor density N_D ($1/cm^3$)	$5.0x10^{16}$	0	$1.0x10^{18}$
shallow uniform acceptor density N_A ($1/cm^3$)	0	$1.0x10^{16}$	1

Table 2. Parameters of back and front contacts that used in SCAPS simulation.

Interface Parameters	Front Contact	Back Contact
Metal work function (eV)	4.472	5.297
Surface recombination velocity of holes ($cm.s^{-1}$)	10^7	10^7
Surface recombination velocity of electrons ($cm.s^{-1}$)	10^7	10^7

Therefore, there will be two competing forces in the p-n junction, diffusion opposed by drift, and the equations of transport of carrier in semiconductors occur by being carried and diffusion as explains below:

$$J_p = qD_p \frac{\dot{dp}}{dx} + q\mu_p pE \tag{4}$$

$$J_n = qD_n \frac{dn}{dx} + q\mu_n nE \tag{5}$$

where the μn has described as electron and μp is as hole mobility. The absorption coefficients of the absorber layer are one of the crucial things in the simulation process. In SCAPS-1D, the optical absorption coefficient can set up from either a file which is this file we may get from literature, and it is in the form of a two-column and saved as input ASCII files and when it is were set from a model, the α(λ) equation as expressed by:

$$\alpha(\lambda) = \left(A + \frac{B}{h\lambda}\right)\sqrt{h\lambda - E_g} \tag{6}$$

where h is Planck's constant, E_g is the bandgap energy, and λ is the wavelength of the incident light. The absorption Coefficient (α) of CuO material that apply to in the present simulation was taken from file or literature, which is the α as expressed in the following equation:

$$\alpha = \frac{4\pi k}{\lambda} \tag{7}$$

Meanwhile, the absorption coefficient value of both materials ZnO and AZO metal oxide was taken from spectrum files as provided in SCAPS Software.

3. Results and discussion

3.1. Investigation of the Effects of Thickness and Carrier Concentration Variation of P-CuO Absorber Metal Oxide on the Device Performances

In this part, the influence of the thickness and carrier concentration variation p-CuO absorber/n-ZnO Window layer have been inspected with the purpose to obtain the qualitative information on the device performance. Here, the carrier concentration of p-CuO as the absorber layer were varied from $1x10^{13}$ to $5x10^{17}$ cm^{-3}, meanwhile the thickness was varied from 10 to110 nm. Furthermore, the band gap energy value of the CuO absorber has been kept constant at 1.5 eV as illustrated in table 1. The result shows that the absorber layer material in solar cell device issue is the crucial issue and it known as the most significant component of the solar cell structure, which through this material the incident photons are absorbed, and finally the extra carriers are generated via this layer. In Fig.2. shows the 2D contour plot displaying the effects of p-CuO layer thickness and carrier concentration variation on the device performance (V_{oc}, J_{sc}, FF, and η). We assume that solar performance is affected by the increasing of Shockley-Read-Hall (SRH) recombination owing to finite carrier diffusion length caused by increasing the thickness of the CuO absorber layer. In thin films solar cell, SRH recombination plays a vital role, which is the SRH recombination rate is as express in the following equation;

$$U = \frac{\sigma_n \sigma p v_{th} N_T (np - {n_i}^2)}{\sigma_n \left[n + n_i \, exp\left(\frac{E_T - E_i}{kT}\right)\right] + \sigma_p \left[p + n_i \, exp\left(\frac{E_i - E_T}{kT}\right)\right]} \tag{8}$$

where, σ are capture cross-sections, v_{th} is described as thermal velocity, N_T and E_T are defect concentration and energy level above the valence band, respectively.

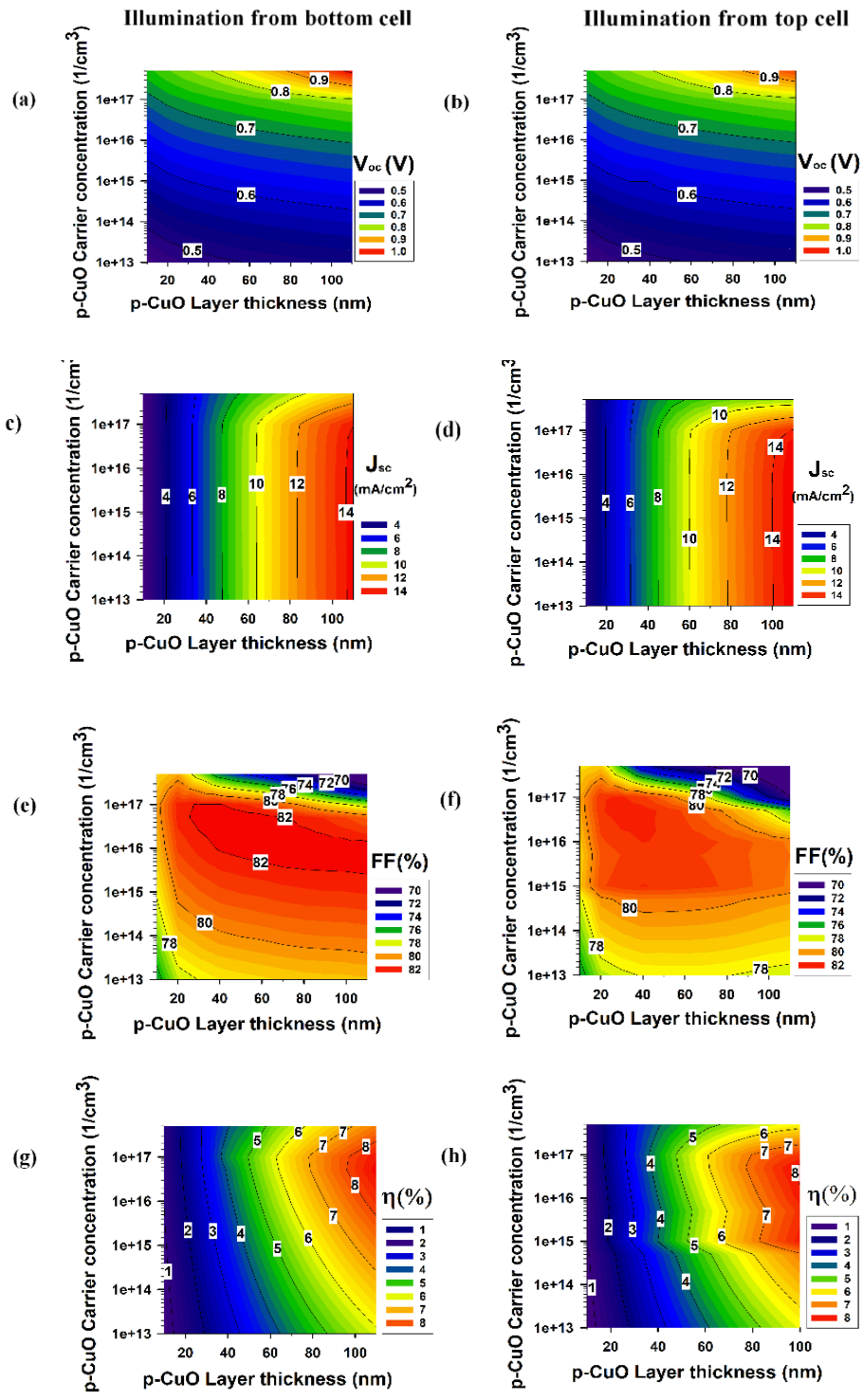

Fig. 2. The 2D contour plots of Semitransparent Thin-film heterojunction solar cell performance by varied 10-110 nm thickness of p-CuO layer, which the n-ZnO thickness and doping/carrier concentration were kept at 200 nm, and $5x10^{16}$ respectively, as illumination from bottom cell and top cell.

These results are following the trend and is consistent with the previous report which attributed to improving the absorption of the incident light, when the thicker of the absorber layer, then more collection of photons are absorbed with a big number of electron hole pairs are generated, and it caused in resulting an increased the photo generated current [28]. It's clearly shown that the higher the absorber layer thickness the better solar cells device performance as

illustrated in Fig.2. Therefore, the CuO absorber layer with a thickness of 110 nm results in the highest efficiency of 8.714 %. The absorber layer thickness is kept thin to overcome the fabrication cost issue, and it is well known that CuO is not a fully transparent material to the visible light spectrum. Hence, it is very important to reduce its thickness to achieve semi-transparent device photovoltaic cell for practical application purposes.

3.2. The Influence of Thickness and Carrier Concentration Variation of n-ZnO Window Layer on the Devices Performance

Zinc oxide is the prominent metal oxide that has been applied in thin film solar cells technology, and it generally was used as a window/buffer layer owing to it have a large bandgap and high optical properties. As theoretically and practically proven that the performance or the characteristic of solar cells devices depends on the band alignment at the hetero interface. The ZnO material with some beneficial properties and of them is it has a large bandgap of 3.3-3.4 eV which allow more photon absorption in the absorber layer. From Fig.3 2D contour plot, we noticed that as the ZnO window layer thickness was set in the range of 10-50 nm the then the Jsc values shows are almost the same for all carrier concentration variation or no significant change of Jsc value for all doping level variation. We found that while the ZnO thickness was set above 50 nm and the doping level at lower condition (below $1x10^{16}$ cm^{-3}) then the jsc values are decreased depending on the thickness and carrier concentration or the doping level.

According to the illustrated 2D contour plots images in fig. 3. it shows the short circuit current density (J_{sc}) was increased as the thickness decrease then following by the improvement of the efficiency of the solar devices as the ZnO window layer carrier concentration or the doping level was set at the highest level ($5x10^{18}$ cm^{-3}). In this case, we assume that the improvement of J_{sc} owing to a better collection of the photo-generated electrons, which influenced the efficiency. Here, the lower thickness is required in conjunction to attain the good efficiency/performance of solar cell structure. We found that 20 nm thick n-ZnO n-type window layer was chosen as the optimized thickness corresponding to a cell efficiency value of 8.9116 %. The thin window layer may help to avoid absorption loss in solar cell devices. Furthermore, the results have shown that the increase in the doping level/carrier concentration of the ZnO window layer may assist in a contrast improvement on the performance of cell devices, and the obtained results following the trend of the previous report. The others result shows that the increase in doping level /carrier concentration and thickness of ZnO window may be affected to reduce of the V_{oc} parameter. In the case of variant doping in our semitransparent structure device model, that the higher doping level/carrier concentration of the ZnO window layer is necessary, and in purpose to immune the window layer thickness variation.

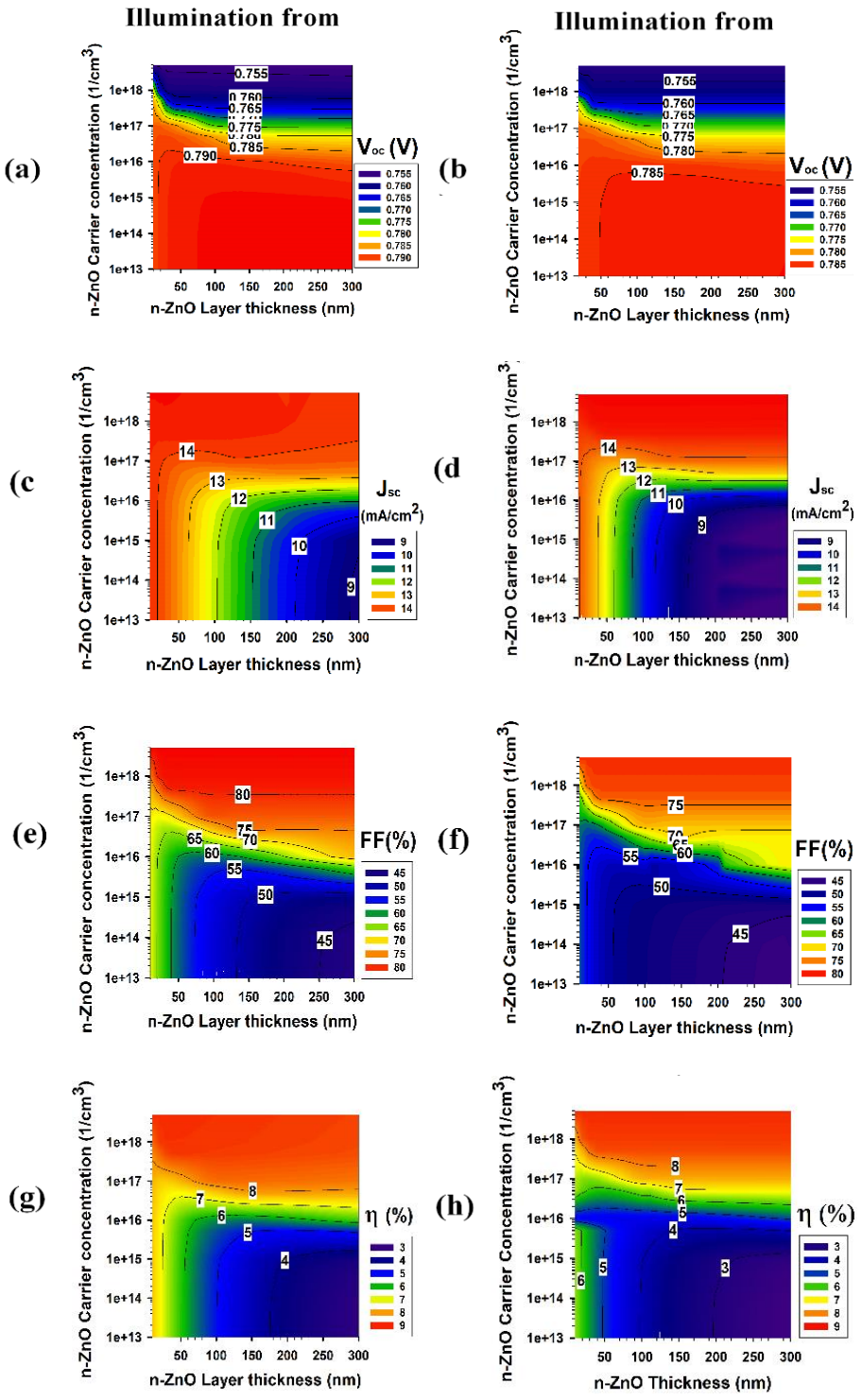

Fig. 3. The 2D contour plots of Thin-film heterojunction solar cell device performance (Voc, Jsc, FF and η), by varied 10-300 nm thickness of n-ZnO layer which the n-ZnO thickness and doping/carrier concentration were kept at 110 nm, and 1x10^{16} respectively, as illumination from bottom cell and top cell.

Moreover, the overall results show that the thicker thickness and low doping level/ carrier concentration of the ZnO window layer may reduce the efficiency of the cells. In a certain case, while the doping level/carrier concentration was set up higher (10^{17} - 10^{18} cm^{-3}) the efficiency getting increase constantly for a whole thickness varied with insignificant changes. These phenomenon results can be explained by relevant theory in term of the free-carrier concentration in an n-type material/semiconductor as expressed:

$$n \approx N_c \; exp\left[-\left(E_c - E_f\right)/kT\right] \tag{9}$$

where, Nc and k are representing an effective density of states in the conduction band and the Boltzmann constant respectively, meanwhile T for absolute temperature. Unlike the p-CuO layer case, whih is the thickness CuO absorber layer has varied from 10 to110 nm, for n-ZnO window layer the varied of thickness higher than it which is in the range 10-300 nm, and experimentally the physical of 300 nm ZnO still in transparent category owing to the ZnO has high transparency. Based on our investigation, the thinner of the n-ZnO window layer was contribute to generating more current as it may increase the performance of solar cell parameters (Voc, Jsc, FF, and η) devices, and as the previous research study was reported that the characteristic solar cells performances depend on the thickness varied of n-ZnO window layer. As observed, 20 nm n-ZnO window layer was chosen as the optimal thickness corresponding to a cell efficiency value of 8.9116 %, and it consistent with the theoretical and experimental results. Note, to minimize the series resistance of the PV device, the thickness of the window/buffer layer should be thin as well.

3.3. Investigation the Influence of varied Carrier Concentration of p-CuO /n-ZnO Layer on the Device Performance

In this part, the varied doping level/carrier concentration on p-CuO absorber and n-ZnO window have been carryout continuing the previous section, in purpose to achieve the best doping for that active layer to support the increasing the performance of semitransparent thin film solar cell devices. Furthermore, the setting parameter CuO absorber doping level/carrier concentration is from 1×10^{16} cm^{-3} to 9×10^{16} cm^{-3}, which the thickness was kept constant at 70 nm. Meanwhile, the n-ZnO window layer thickness and the doping level are being keep constant at $5x10^{17}$ cm^{-3} and 200 nm thick respectively. According to the simulation results calculation, the V_{oc} increase rapidly for all variant exponential value throughout as the doping increased and as show in fig. 4(a), however for the J_{sc}, η, and the fill factor were an increase in the lower doping level but at a certain point it those parameters starts decreasing along with the absorber layer (CuO) doping level/carrier concentration value increased. These simulated results are consistent and in accordance with the simulation and experimental results from some other group research mentioned an increase in the doping level/carrier concentration may reduce the minority carrier lifetime, which means by implying more recombination and thus, reducing the collection of charge carriers at the contacts [28,37,38]. The optimized doping/carrier concentration for p-CuO absorber layer of 6 $x10^{16}$ cm^{-3} which corresponds to the obtained the cell efficiency of 8.7209 %.

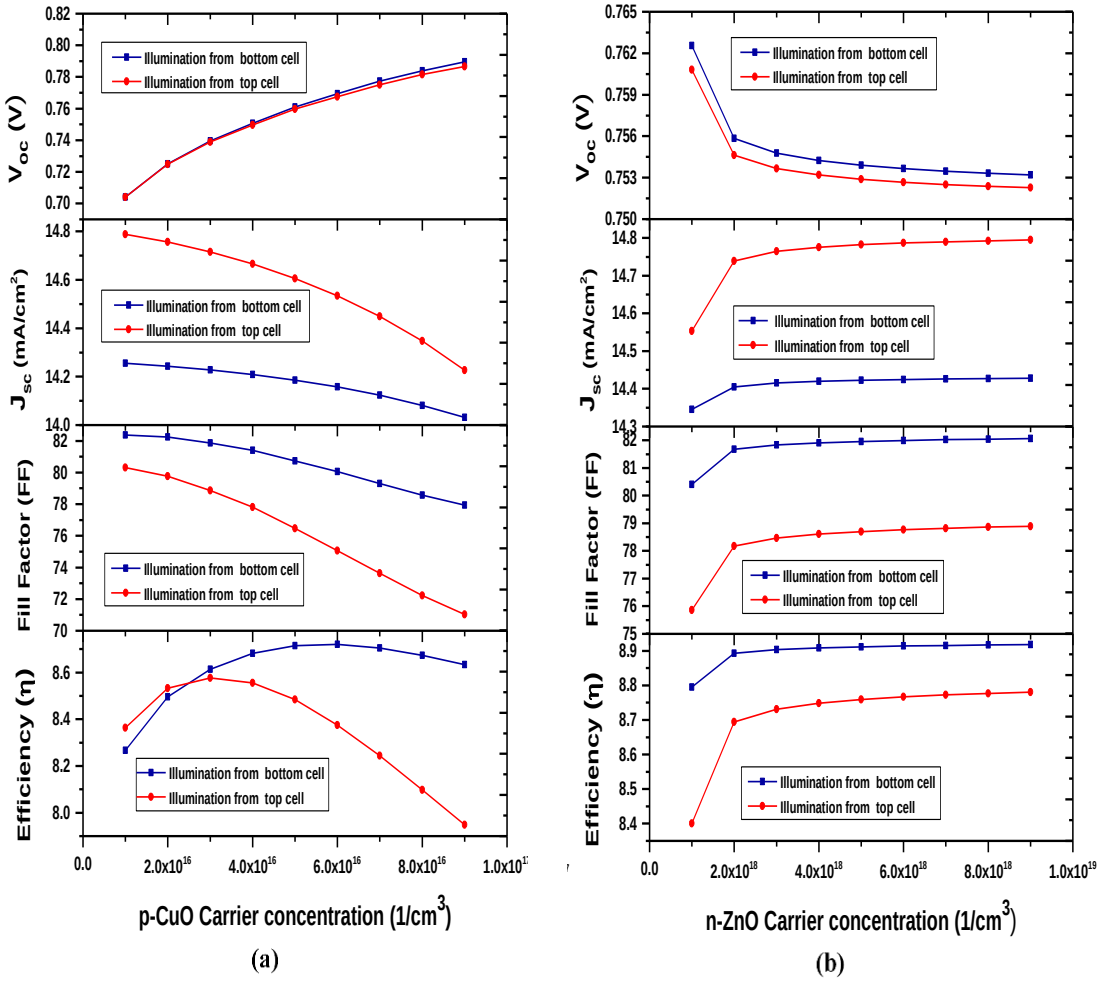

Fig.4. (a and b). Thin film heterojunction of p-CuO/n-ZnO Solar cells Device Performance plots Curve (J_{sc},V_{oc}, FF and η) as the illumination from bottom cell and top cell, through varied carrier concentration of n-ZnO and p-CuO layer.

Theoretically, decrease in the reverse saturation current, J_o, results in the increase of open circuit voltage (V_{oc}) value. This fact can be explained by Shockley equation as express bellow;

$$V_{oc} = \frac{KT}{q} In\left(\frac{J_{ph}}{J_0} + 1\right) \tag{10}$$

where, T is being defined as the operating temperature, K is for the Boltzmann constant, and q is the symbol for the elementary charge, while J_{Ph} and J_0 are were described as the photo-generated current density and the saturation current density respectively. Further, for the saturation current density (J_0) as described in the following expression:

$$J_0 = An_i^2 \left(\frac{D_e}{L_e N_A} + \frac{D_h}{L_h N_D}\right) \tag{11}$$

Here, n_i is the intrinsic carrier concentration; the electrons and holes diffusion coefficient are being dined as D_e and D_h respectively. For L_e and L_h are the electrons and holes diffusion length, respectively, while the N_A and N_D are the acceptor concentration and donor concentration respectively, and finally A is the diode quality factor.

The varied of doping level ZnO window layer is in the range of $1x10^{18}$ cm^{-3} to $9x10^{18}$ cm^{-3}, while the thickness kept constant at 20 nm. Meanwhile, for CuO doping level and the thickness are being kept constant at 6 $x10^{16}$ cm^{-3} and 110 nm respectively. As Fig.4b. show the higher doping concentration on the n-ZnO window layer, the better the performance of the device.

As illustrated in Fig. 4(b) the current results seem opposite than results in fig. 4(a). The results were described that the higher doping gave the good influence in particular on the characteristic/parameters (J_{sc}, V_{oc}, FF, and η) of the cell devices. As overall show that the performances of the cells have been generated dependent on the doping/carrier concentration variation of the n-ZnO window layer. In the other hand, it is shows the open circuit voltage (V_{oc}) increase as doping decreased and continuing low when the n-ZnO window layer dopin/carrier concentration increased. We note, to maintain the higher doping for the n-ZnO window layer, which may assist for low V_{oc} and can contribute the good or better performance for others parameters (Jsc, FF, and η) as well. Finally, we found that the optimized doping or carrier concentration of ZnO n-type window layer were chosen at 9 x10^{18} cm^{-3} which corresponding to a cell efficiency of 8.9178 %.

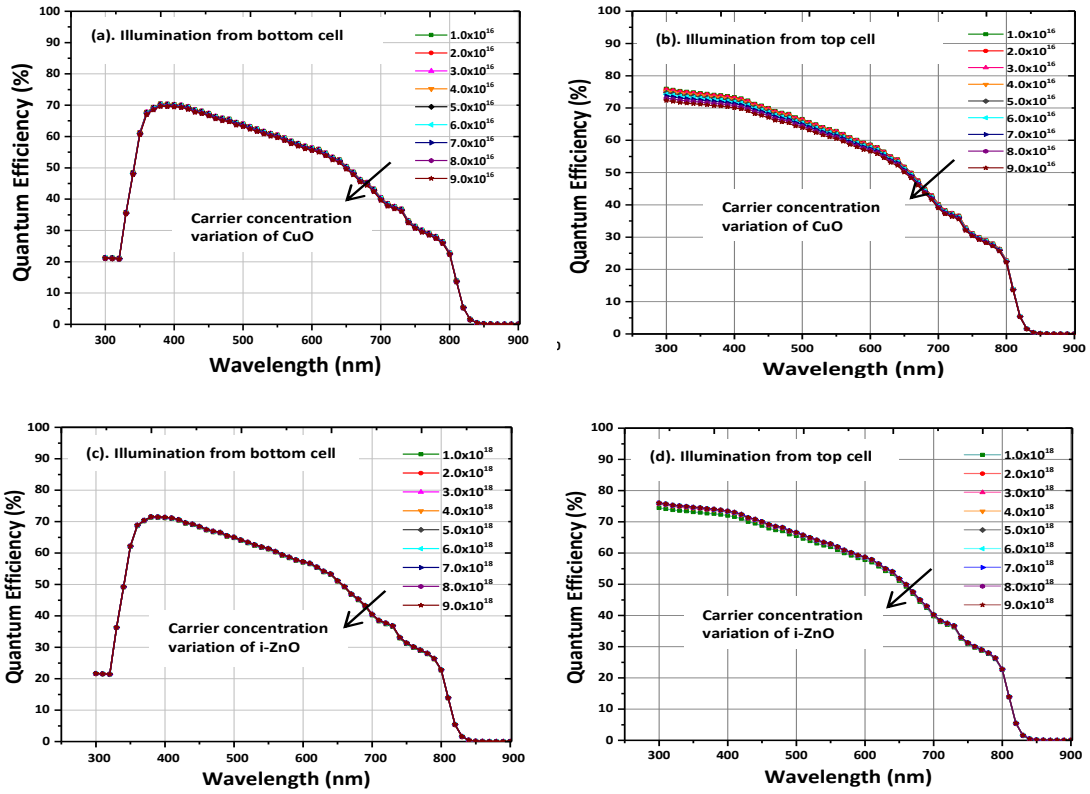

Fig. 5. (a,b.c and d) Quantum Efficiency of of thin film heterojunction of solar cells Structure by varied Carrier concentration of p-CuO/n-ZnO layer, as the illumination from bottom cell and top cell

Fig. 5 shows the quantum efficiency of thin film heterojunction of p-CuO/n-ZnO/AZO/ITO semitransparent thin films heterojunction solar cells as the p-CuO absorber/n-ZnO window with the configuration (doping and thickness) as mentioned in the previous section. The result show that good QE were achieved especially in the range of short wavelength region (300 nm to 510 nm). This result was mainly influenced by ZnO metal oxide which has a large band gap (3.34 eV) and transparent which caused a good response to the solar shortwave spectrum. Definitely, the wide band-gap of ZnO films caused more photons to be transmitted into the CuO absorber film. Hence, more photo-generated carriers were produced in the CuO film, and consequently the short-circuit current density automatically was improved. Furthermore, there is no significant change has been found in QE performance while the CuO absorber and ZnO window layer were varied in different carrier concentration as seen in Fig.5. Based on our investigation, the performance of solar cell parameters which illumination was set from the bottom cell has a better performance compared to the cell with illumination from the top cell. Although, this condition was achieved in a certain case, where the CuO absorber layer was set at a thickness

below 110 nm, we found the percentage of efficiency was increase significantly while the light set up or the illumination from the bottom side. However, continued research numerically and experimentally regarding this issue is necessary.

4. Conclusions

In this work, a semitransparent thin film heterojunction solar cells device structure of p-CuO/n-ZnO/AZO/ITO was numerically modeled using SCAPS-1D software tools. The cell's performance was investigated in terms of the different material layer properties, such as the thickness and carrier concentration or doping level. Our findings reveal that the best value for thickness and doping/carrier concentration of n-ZnO window layer in our present model structure are 20 nm and $9x10^{18}$ cm^{-3} correspondingly, which is considering as the optimized parameter and corresponding to cell efficiency result of 8.9178 %. We believe the optimised p-CuO/n-ZnO thickness and doping concentration values obtained in this work can reduce or minimize the cost fabrication this metal oxide TFSC for semi-transparent thin film solar cell applications.

Acknowledgments

The SCAPS (3.3.07) simulation software used in this study was provided by Marc Burgelman, University of Gent, Belgium. We acknowledge the technical support given by Institute of Microengineering and Nanoelectronics (IMEN), UKM. This research was funded by ASEAN India S&T Development Fund (AISTDF) (RR-2020-002).

References

[1] J. Sun, J. J. Jasieniak, J. Phys. D: Appl. Phys. **50**, 1 (2017).
[2] Dong Hee Shin, Suk-Ho Choi, Coatings **329**(8), 1 (2018).
[3] K. L. Chopra, P. D. Paulson, V. Dutta, Thin-film solar cells **12**, 69 (2004).
[4] C. W. Tang, Appl. Phys. Lett. **48**, 183 (1986).
[5] G. Yu, J. Gao, J. C. Hummelen, F. Wudl, A. J. Heeger, Science **270**, 1789 (1995).
[6] J. J. M. Halls, C. A. Walsh, N. C. Greenham, E. A. Marseglia, R. H. Friend, S. C. Moratti, A. B. Holmes, Nature **376**, 498 (1995).
[7] B. O'Regan, M. Grätzel, Nature **353**, 737 (1991).
[8] M. M. Lee, J. Teuscher, T. Miyasaka, T. N. Murakami, H. J. Snaith, Science **338**, 643 (2012).
[9] C. G. Granqvist, Appl. Phys. A **57**, 19 (1993).
[10] B. K. Meyer, A. Polity, D. Reppin, M. Becker, P. Hering, P. J. Klar, T. H. Sander, C. Reindl, J. Benz, M. Eickhoff et al, Phys. Status Solidi B **249**, 1487 (2012).
[11] A. H. Jayatissa, K. Guo, A. C. Jayasuriya, Appl. Surf. Sci. **255**, 9474 (2009).
[12] R. H. Bari, S. B. Patil, A. R. Bari, International Nano Lett. **3**, 2013.
[13] Ş. Korkmaz, B. Geçici, S. D. Korkmaz, R. Mohammadigharehbagh, S. Pat, S. Özen, G. Yudar, Vacuum **131**, 142 (2016).
[14] T. V. Pham, M. Rao, P. Andreasson, Y. Peng, J. Wang, K. Jinesh, Appl. Phys. Lett. **102**, 032101 (2013).
[15] M. Heinemann, B. Eifert, C. Heiliger, Phys. Rev. B **87**, 115111 (2013).
[16] N. Serin, T. Serin, Ş. Horzum, Y. Celik, Semicond. Sci. Technol. **20**, 398 (2005).
[17] V. Figueiredo, E. Elangovan, G. Goncalves, P. Barquinha, L. Pereira, N. Franco, E. Alves, R. Martins, E. Fortunato, Appl. Surf. Sci. **254**, 3949 (2008).
[18] P. A. Korzhavyi, B. Johansson, (2011) SKB-TR–11-08 Swedish Nuclear Fuel and Waste Management Co.1
[19] S. C. Ray, Sol. Energy Mater. Sol. Cells. **68**, 307 (2001).
[20] N. M. Shanid, M. A. Khadar, Thin Solid Films 516, 6245 (2008).
[21] H. Kidowaki, T. Oku, T. Akiyama, J. Phys. Conf. Ser. **352**, 012022 (2012).
[22] A. Kaphle, E. Echeverria, D. N. Mcllroy, P. Hari, RSC Adv. **10**, 7839 (2020).

[23] H. Siddiqui, M. R. Parra, P. Pandey, M. S. Qureshi, F. Z. Haque, Advanced Materials and Devices **5**, 104 (2020).
[24] Minami, Y. Nishi, T. Miyata, Appl. Phys. Express **9**, 052301 (2016).
[25] P. Hu, W. Du, M. Wang, H. Wei, Jun Ouyang, Zhao Qian, Yun Tian. J. Appl. Phys. **128**, 125302 (2020).
[26] Le Zhu, Guosheng Shao, J. K. Luo. Semicond. Sci. Technol. **28**, 055004 (2013).
[27] V. Kumar, S. Masudy-Panah, C. C. Tan, T. K. S. Wong, D. Z. Chi, G. K. Dalapati, IEEE International Nanoelectronics Conference, 443 (2013).
[28] P. Sawicka-Chudy, Z. Starowicz, G. Wisz, R. Yavorskyi, Z. Zapukhlyak, M. Bester, Ł. Głowa, M. Sibiński, M. Cholewa, Mater. Res. Express. **6**, 085918 (2019).
[29] Terence K. S. Wong, Siarhei Zhuk, Saeid Masudy-Panah, Goutam K. Dalapati, Materials **271**(9), 1 (2016).
[30] Paulina Sawicka-Chudy, Maciej Sibiński, Grzegorz Wisz, Elżbieta RybakWilusz, Marian Cholewa. Journal of Physics: Conf. Series **1033**, 012002 (2018).
[31] P. Mahajan, A. Singh, S. Arya, J. Alloys Compd. **814**, (152292 2019).
[32] J. Schrier, D. O. Demchenko, L. Wang, A. P. Alivisatos, Nano Lett. **7**, 2377 (2007).
[33] Giovanna Sozzi, Fabrizio Troni, Roberto Menozzi. Solar Energy Materials & Solar Cells **121**, 126 (2014).
[34] R. Scheera. Journal of Applied Physics **105**, 104505 (2009).
[35] Helena Wilhelm, Hans-Werner Schock, Roland Scheer. Journal of Applied Physics **109**, 1 (2011).
[36] F. Anwar, S. Sarwar Satter, R. Mahbub, S. Mahmud Ullah, S. Afrin, Journal of Renewable Energy Research **7**, 885 (2017).
[37] D. Smazna, S. Shree, O. Polonskyi, S. Lamaka, M. Baum, M. Zheludkevich, F. Faupel, R. Adelung, Y. K. Mishra, Journal of Environmental Chemical Engineering **7**, 103016 (2019).
[38] R. Singh, S. Dutta, Nano-Structures & Nano-Objects **18**, 100250 (2019).